Experimental and Density Functional Theory Study of the Vibrational Properties of 2-Mercaptobenzimidazole in Interaction with Gold

Th. Doneux,[†] F. Tielens,[‡] P. Geerlings,[§] and Cl. Buess-Herman*,[†]

Service de Chimie Analytique et Chimie des Interfaces, Université Libre de Bruxelles, Boulevard du Triomphe 2, CP 255, 1050 Bruxelles, Belgium, Laboratoire de Chimie Théorique, Université Pierre et Marie Curie, Paris VI, 4 Place Jussieu, Boîte 137, F-75252 Paris, Cedex 05, France, and Fakulteit Wetenschappen, Algemene Chemie, Vrije Universiteit Brussel, Pleinlaan 2, B-1050 Brussels, Belgium

Received: March 14, 2006; In Final Form: July 7, 2006

The vibrational properties of the 2-mercaptobenzimidazole (MBI) molecule in interaction with gold were examined by a combined approach of FTIR measurements and density functional theory (DFT). A complete assignment of the 42 normal modes of MBI has been performed on the basis of DFT calculations at the B3PW91 level in complement to the Raman and FTIR spectra. Calculations demonstrated that, on the deprotonated MBI molecule, the negative charge is localized on the sulfur atom, favoring the formation of a gold−sulfur bond upon reaction of MBI with gold. This was confirmed by the very good agreement between the calculated spectrum and the experimental spectra of different gold−MBI compounds, indicating that the vibrational properties of adsorbed MBI are chiefly determined by the coordination through the sulfur atom.

1. Introduction

The combination of electrochemical and in-situ infrared spectroscopic techniques is nowadays widely applied to describe the metal−solution interfaces. Especially, the so-called subtractively normalized interfacial Fourier transform infrared spectroscopy (SNIFTIRS) has been proved to be a powerful technique to describe the adsorption of organic molecules on metal substrates.[1−3] This method has been recently used by us to study the adsorption behavior of the 2-mercaptobenzimidazole (MBI) molecule on a Au(111) electrode.[4,5]

The self-assembled monolayer of MBI was characterized by electrochemical techniques and SNIFTIR spectroscopy,[4] and it was shown that the MBI molecule is adsorbed through the formation of a gold−sulfur bond and can be electrochemically desorbed either in a neutral or an anionic form depending on the pH of the solution. Despite the fact we were able to get an experimental infrared spectrum of the anionic form of MBI, the bands assignment was difficult since, to our knowledge, no IR data were available in the literature concerning anionic MBI.

In a subsequent study, the effect of the electrode potential on the amount and the orientation of the MBI at the surface has been examined.[5] To get good quality spectra, with a high signal-to-noise ratio even for a submonolayer amount of MBI, the experiments were performed in deuterated water. Figure 1 presents a typical SNIFTIR spectrum, in deuterated water, compared to the spectra of anionic and neutral MBI in deuterated solvent. The positive bands of the SNIFTIR spectrum exactly match those of anionic MBI, while the negative bands display patterns similar to the spectrum of neutral MBI. Due to the presence of two labile hydrogen atoms on the nitrogen atoms of the molecule, the infrared spectrum of MBI strongly differs in hydrogen or deuterium media, and the bands assignment was again not straightforward.

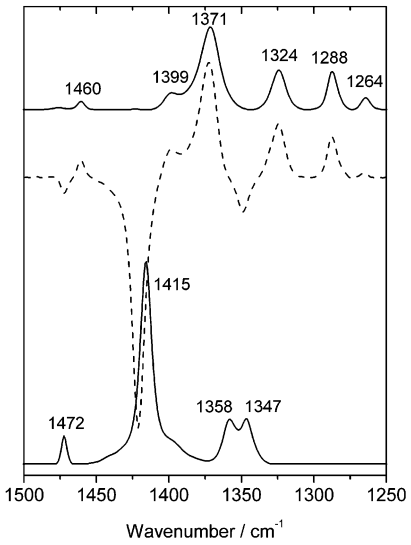

Figure 1. Comparison of a SNIFTIR spectrum (dashed line) to the absorbance spectra of MBI dissolved in deuterated methanol (bottom, solid line) and in D_2O + NaOH (top, solid line). The SNIFTIR spectrum displayed on the figure is that obtained at the sample potential of −0.3 V. Under the experimental conditions used, negative bands reflects the spectrum of the adsorbed monolayer, while positive bands are due to desorbed species. From ref 5.

This work is aimed at getting reliable information on the vibrational properties of MBI and some of its derivatives and on the interaction between MBI and a gold surface, using density functional theory (DFT) calculations. DFT has been successfully applied to the description of the vibrational properties of many molecules, including heterocycles.[6−8]

Figure 2 presents the structures of the compounds whose spectra were calculated: MBI, the anionic form of MBI, a gold complex of MBI, and their deuterated isotopomers.

* Corresponding author. Tel: + 32 2 6502939. Fax: + 32 2 6502934. E-mail: cbuess@ulb.ac.be.
[†] Université Libre de Bruxelles.
[‡] Université Pierre et Marie Curie.
[§] Vrije Universiteit Brussel.

10.1021/jp061582v CCC: $33.50
Published on Web 09/08/2006

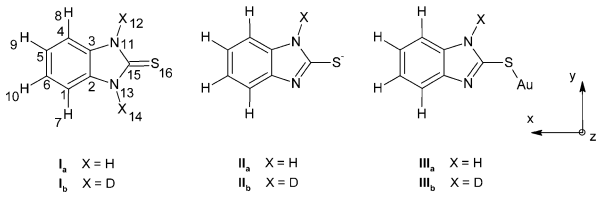

Figure 2. Structures of the investigated compounds.

The DFT calculated spectra of these species were compared to experimental spectra to gain some insight in the interaction of MBI with gold at the electrochemical interface.

2. Experimental Section

2-Mercaptobenzimidazole (98%, Acros) was recrystallized in absolute ethanol (Merck). KBr (for spectroscopy, Merck) was dried at 110° before use. Deuterated methanol (CD_3OD, 99.8+%, Aldrich), deuterium oxide (99.9%, Cambridge Isotope Laboratories), $AuCl_3$ (Alfa Aesar), NaOH (Pro Analysi, Carlo Erba), and HCl (Pro Analysi, Chem-Lab) were used as received.

The Raman spectrum of MBI was recorded directly on the finely grinded solid with a Perkin-Elmer Spectrum 2000 FT-Raman spectrometer using a red-light Nd:YAG laser (25 mW) emitting at 1064 nm. A total of 128 scans were collected at a 4 cm^{-1} resolution. The infrared spectra were collected with a Nicolet 20DXB spectrometer equipped with a DTGS detector. IR spectra of solutions as well as solids dispersed into KBr pellets were recorded. For the solutions, a thin layer cell consisting in two flat IR windows (CaF_2 or ZnSe) separated by a 25 μm thick Teflon spacer was used. The solution spectra of MBI (in methanol solvent), N,N′-dideuterated MBI (in CD_3OD), anionic MBI (in H_2O + NaOH, pH > 12.5), and deuterated anionic MBI (D_2O + NaOH, pH > 12.5) were obtained. Due to the low concentration of MBI in solution (~1% w/w), the H−D exchange is assumed to be complete in the deuterated solvents. KBr pellets were employed for solid MBI and for gold−MBI compounds.

Compounds were synthesized in two different ways. The first one (AuMBI-1) was prepared by mixing a 10^{-3} M $AuCl_3$ + 10^{-1} M HCl aqueous solution with a 10^{-3} M MBI aqueous solution, in a ratio 1:3. A white precipitate was obtained which was isolated, rinsed, dried, and dispersed in KBr.

The second one (AuMBI-2) was prepared by mixing the same solutions in the presence of $NaBH_4$. The reaction product was a colloidal suspension of MBI-capped gold aggregates. The particules were coagulated, rinsed, dried, and finally dispersed in KBr. For each spectrum 800 scans were collected at a resolution of 2 cm^{-1}.

3. Computational Details

To calculate the vibrational frequencies of the MBI molecule before and after interaction with gold, a density functional theory (DFT)[9,10] approach was used by means of the B3PW91 functional,[11] which has proven its reliability,[10,12] in combination with the LanL2DZ pseudopotential[13−15] enabling one to obtain good quality geometries, interaction energies, and vibrational frequencies as was shown in former studies.[16,17] These calculations were carried out with the Gaussian98 program.[18]

The generally good performance of the hybrid functionals such as B3PW91 and B3LYP for frequencies has been discussed in ref 19. DFT intensities calculated at this level may be considered to be of reliable certainty when a semiquantitative spectral intensity pattern is required.[10,20] In our study we limited the calculation level to the B3PW91/pseudopotential level, which as will be seen gives satisfactory results.

The MBI molecule and anion were fully optimized for their hydrogen and deuterium isomers. The interaction was simulated using a single gold atom (see Figure 2).

4. Results and Discussion

4.1. 2-Mercaptobenzimidazole Molecule. *4.1.1. Molecular Parameters.* The X-ray structure of 2-mercaptobenzimidazole molecule (compound $\mathbf{I}_a$ in Figure 2) in the solid state has been determined already in the 1970s by Form and Raper[21] and was confirmed later by Murty[22] and Ravikumar.[23] A tautomeric equilibrium between the thione and the thiol form exists, but many works, including a semiempirical gas phase study,[24] have shown that the thione form of MBI is predominant. In the solid state, the molecules form long H-bonded chains along the *b* axis of the crystal, which corresponds to the *y* axis of Figure 2. The comparison between the experimental and calculated structure results in a good correlation, characterized by correlation coefficients values of 0.9854 and 0.9167 for the bond lengths and bond angles, respectively. The largest deviations are observed for bond lengths and bond angles involving the hydrogen atoms, which is often the case in DFT calculations.[10] It is also possible that these differences originate from the fact that the experimental data were obtained for solid state MBI, where intermolecular interactions such as H-bonding occurs, while the calculations were performed for a single molecule. If the comparison is restricted only to the skeleton C and N atoms and to the exocyclic S atoms, the correlation coefficients are 0.9987 and 0.9965, respectively, which are more accurate than those obtained in other works on heterocyclic molecules.[8,25]

A permanent dipole moment is found to be oriented along the *x* axis; its calculated value amounts to 5.07 D. An experimental value of 4.1 D, measured for MBI dissolved in benzene or dioxane, has been previously reported by Cumper and Pickering.[26]

4.1.2. Vibrational Analysis. MBI is a heterocyclic molecule composed of 16 atoms, having two planes of symmetry (the *xy* plane and the *xz* plane; see Figure 2) and a C_2 axis of symmetry (the *x* axis), and belongs to the C_{2v} point group. A total of 42 vibrations are then expected for MBI, distributed as follows:

$$\Gamma_{vib} = 15\,A_1 + 6\,A_2 + 7\,B_1 + 14\,B_2 \qquad (1)$$

Normal coordinates having A_1 and B_2 symmetry are assigned to symmetric and antisymmetric in-plane vibrations, oriented along the *x* axis and *y* axis, respectively. Similarly, the out-of-plane symmetric vibrations belong to B_1 symmetry and are oriented along the *z* axis, while the A_2 modes, which are not active in infrared spectroscopy but are active in Raman scattering, correspond to out-of-plane antisymmetric vibrations. Experimental vibrational analyses of MBI have been already reported in the literature.[27−30] Especially, the study of Bigotto[28] provides an extensive description to which we can refer in this work.

Figure 3 presents the Raman, FTIR, and calculated IR spectra of 2-mercaptobenzimidazole. The unscaled calculated spectrum is represented in the stick form. A detailed analysis of the spectra is given in Table 1. The table presents the experimental and unscaled calculated wavenumbers together with the calculated intensities, irreducible representations, and assignments.

The experimental wavenumbers reported in the second column were obtained from the different available spectra of MBI, i.e., Raman, solid FTIR, and methanolic solution FTIR

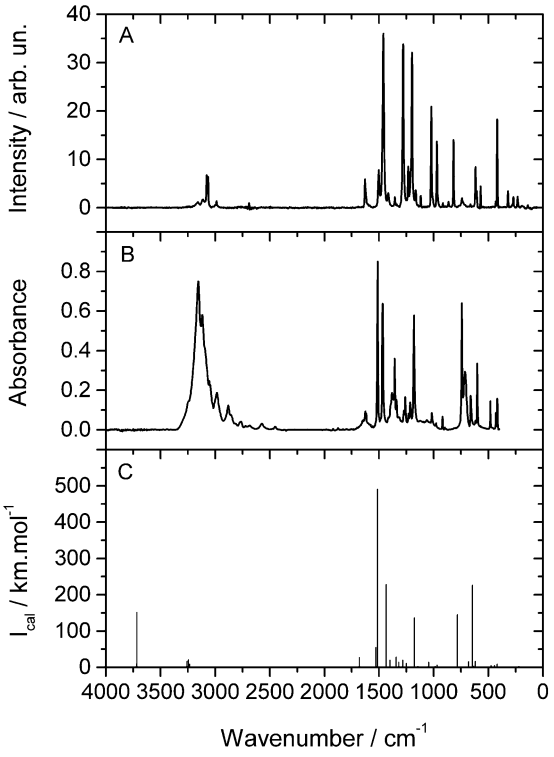

Figure 3. Vibrational spectra of 2-mercaptobenzimidazole: A, experimental Raman scattering spectrum; B, experimental infrared absorption spectrum; C, calculated infrared absorption spectrum, presented in the stick spectrum form.

spectra. The missing rows of this column correspond to bands which were not observed in any experimental spectrum. This is not so surprising considering that for all these bands the calculated IR intensities are found to be very small. The third column of Table 1 presents the wavenumbers as they were calculated at the B3PW91 level. It is common to apply a scaling factor to the calculated wavenumbers to get a better correlation between the experimental and theoretical spectra.[31,32] The use of this scaling factor as well as the scaling value is still an open question and is not the topic of this work. However, we may compare the ratio $R = \nu_{exp}/\nu_{calc}$ obtained here with results reported in the literature. In the high-frequency region (>2500 cm^{-1}), small values of R, around 0.84 for the NH stretchings and 0.94 for the CH stretchings, are found. In the wavenumber range between 500 and 2500 cm^{-1}, the R values are just below unity, and their mean value equals 0.979. In the low-frequency range (<500 cm^{-1}), R tends to be slightly larger than 1. This trend is in good agreement with other combined DFT and experimental studies on small organic and heterocyclic molecules.[32]

Vibrations above 3000 cm^{-1} are easily assigned to NH and CH stretching vibrations. One of the CH stretching is not experimentally observed, as expected from the zero intensity calculated by DFT. The bands located on the experimental IR spectrum between 3000 and 2500 cm^{-1} are overtones and combination bands. The 2980 cm^{-1} band most probably results from a Q9 + Q11 combination.

Out-of-plane CH bendings (τ(CH)) are relatively easy to identify. The very intense band at 741 cm^{-1} is a characteristic pattern of a 1,2-disubstituted benzene ring.[33] According to Bigotto,[28] the other τ(CH) are assigned to the bands centered at 916, 955, and 864 cm^{-1}. The last one has an A_2 symmetry and is thus inactive for infrared spectroscopy but is clearly observed on the Raman spectrum.

The NH out-of-plane bendings (τ(NH)) were calculated at 645 and 621 cm^{-1} for the symmetric and antisymmetric modes, respectively. The available IR experimental studies of MBI fully agree to assign the symmetric τ(NH) to the broad band observed at 713 cm^{-1} whose large intensity is correctly reflected by the calculation. As expected from the A_2 symmetry of the antisymmetric mode, no corresponding band is observed on the infrared spectrum. The Raman spectrum displays an additional band at 618 cm^{-1}, but taking into account the measured scaling factor corresponding to the symmetric mode, the experimental vibration should be expected around 680 cm^{-1}. The Raman vibration at 618 cm^{-1} was then assigned to the Q32 mode, whose intensity is predicted to be very small in infrared.

On the basis of the "selenation technique", Devillanova and Verani[27] have identified the vibrations containing a significant contribution from the C═S bond at 661, 601, 482, 419, and 232 cm^{-1}. The huge shift of the 419 cm^{-1} band upon selenation reflects a strong contribution from the C═S stretch, which is in agreement with the results of Bigotto[28] and with the present calculations. Our results provide a more precise assignment of the modes Q34 at 601 cm^{-1} and Q31 at 661 cm^{-1} to in-plane and out-of-plane cycle deformations (torsion) coupled with heavy C═S contributions.

Very strong couplings exist when a C═S bond is attached to one or two nitrogen atoms, as was demonstrated by Rao and Venkataraghavan.[34] They identified characteristic features corresponding to such structures, which they proposed to call "−N−C═S" I, II, and III bands. Harrison and Ralph attributed the peak at 1513 cm^{-1} to the "−N−C═S I" band and the very intense one at 1180 cm^{-1} to the "−N−C═S III" band.[30] This band was also mentioned in other DFT and experimental works for molecules whose structure is close to that of MBI. In the case of 2-thiobarbituric acid, Ramondo et al.[7] identified the band at 1146 cm^{-1} as a coupling between ν(C═S), δ(NH), and ν(CN). Alcoléa Palafox et al.[6] attributed the vibration of 2-thiouracil at 1148 cm^{-1} to the ν(C═S) mode.

The CH in-plane bendings (δ(CH)) are calculated at 1046, 1145, 1208, and 1399 cm^{-1}. The first and second one are attributed according to Bigotto[28] to the bands observed at 1022 and 1119 cm^{-1}, respectively. The last two fall in a spectral range where a lot of couplings exist between skeletal vibrations (C−N and C−C stretchs) and CH and NH in-plane bendings and are less obvious to assign. However, on the basis of the R value of the other δ(CH) and the predicted zero intensity, the Q19 mode can be safely assigned to the Raman active vibration observed at 1164 cm^{-1}. The Q13 mode is attributed to the band at 1359 cm^{-1}.

The C−N stretchings are deeply involved in the A_1 mode at 1280 cm^{-1} and the B_2 mode at 1214 cm^{-1}, while the vibration at 1346 cm^{-1} is mainly due to SCN angular deformations. The calculations indicate that the band at 1234 cm^{-1} contains a huge contribution of the NH in-plane antisymmetric bendings, and that the symmetric fundamental at 1628 cm^{-1} is an almost pure skeletal vibration.

4.2. Benzimidazole-2-thiolate Anion. The acido−basic behavior of 2-mercaptobenzimidazole is characterized by a pK_a value of 10.4.[35] Two resonance forms of the deprotonated MBI exist, represented in Figure 4.

The optimized geometry strongly suggests that the thiolate form (i.e. with the charge localized on the sulfur) is favored. While the two C_{15}−N bonds have the same length, 1.387 Å, in compound **I**, the C_{15}−N_{11} bond length in compound **II** is increased to 1.422 Å and that of the C_{15}−N_{13} bond is decreased to 1.361 Å, consistently with a more pronounced double bond

TABLE 1: Assignments of the 42 Normal Modes of 2-Mercaptobenzimidazole[a]

mode	ν_{exp}/cm^{-1}	$\bar{\nu}_{calc}/cm^{-1}$	$I_{calc}/km\cdot mol^{-1}$	irr rep	assgnt
Q1	3160	3715	151	B_2	ν(NHas)
Q2	3111	3718	9	A_1	ν(NHs)
Q3	3093	3258	15	A_1	ν(CH)
Q4	3054	3245	21	B_2	ν(CH)
Q5	3043	3233	8	A_1	ν(CH)
Q6		3222	0	B_2	ν(CH
Q7		1690	1	B_2	ν(CC)
Q8	1628	1678	26	A_1	ν(CC)
Q9	1513	1529	55	A_1	ν(CC) + ν(CN) + δ(NH)
Q10		1527	0	B_2	ν(CC)
Q11	1467	1515	491	A_1	ν(CC) + ν(CN) + δ(NH)
Q12	1415	1433	228	A_1	ν(CC) + ν(CN)
Q13	1359	1399	20	B_2	δ(CH)
Q14	1346	1343	28	B_2	β(SCN)
Q15	1280	1320	14	A_1	ν(CN)
Q16	1234	1283	19	B_2	δ(NH)
Q17	1214	1250	11	B_2	ν(CN)
Q18	1180	1176	136	A_1	ν(CS) + β(NCN) + δ(NH)
Q19	1164	1208	0	A_1	δ(CH)
Q20	1119	1145	2	B_2	δ(CH)
Q21	1022	1046	14	A_1	δ(CH)
Q22	978	985	2	A_1	β(NCN)
Q23	955	1016	0	A_2	τ(CH)
Q24	916	968	6	B_1	τ(CH)
Q25	898	908	0	B_2	β(CCC)
Q26	864	891	0	A_2	τ(CH)
Q27	819	829	0	A_1	β(CCC)
Q28	741	782	145	B_1	τ(CH)
Q29		780	0	A_2	τ(CCCC)
Q30	713	645	226	B_1	τ(NHs)
Q31	661	680	15	B_1	τ(CNCC) + τ(SCNN)
Q32	618	632	3	B_2	β(CCC) + β (NCC)
Q33		621	0	A_2	τ(NHas)
Q34	601	619	16	A_1	β(NCN) + β(CCC) + ν(CS)
Q35	571	590	0	A_2	τ(CCCC)
Q36	482	473	4	B_2	δ(C═S) + β(NCC)
Q37	432	443	5	B_1	τ(CCCC)
Q38	419	419	8	A_1	ν(C═S)
Q39	321	312	1	B_1	τ NCCC
Q40	271	248	0	A_2	τ(CCCC) + τ(NCCN)
Q41	232	220	2	B_2	δ(C═S)
Q42	116	109	0	B_1	τ(SCNN)

[a] The observed and calculated wavenumbers, calculated intensities, symmetries, and approximate description of each mode are indicated: ν, stretching; δ, β, in-plane bending; τ, out-of-plane bending.

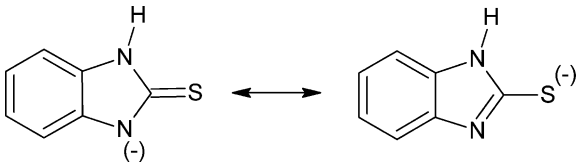

Figure 4. Structure of the resonant forms of anionic MBI.

character. Accordingly, the length of the $C_{15}-S$ bond increases from 1.708 to 1.751 Å. For argument's sake, the characteristic length expected for a C−N single bond is 1.479 Å but 1.352 Å in heterocycles such as pyridine. In the case of carbon−sulfur distances, a single C−S bond measures 1.81 Å and a double C═S bond 1.71 Å.[36] Additionally, the examination of the Mulliken charge distribution on the molecule confirms the very negative character of the sulfur atom, contrary to the N_{13} atom which is almost uncharged.

The deprotonation of the molecule has a significant effect on the vibrational properties of the molecule. The number of atoms being now equal to 15, only 39 vibrations are expected. Concomitantly, compound **II** has only one plane of symmetry (the *xy* plane on Figure 2) and belongs then to the C_s point group. The vibrations are then distributed as $\Gamma_{vib} = 27\ A' + 12\ A''$. The orientation of the transition dipole moments is now less obvious. The A″ species are oriented along the *z* axis, but the A′ species can be oriented anywhere in the *xy* plane. In comparison with neutral MBI, the three missing vibrations can be roughly attributed to one NH out-of-plane bending, one NH in-plane bending, and one NH strectching.

Outside the 1100−1600 cm^{-1} range, the most striking modifications are observed for the frequencies associated to the CH vibrations. The ν(CH) bands are red-shifted by about 40 cm^{-1}, the τ(CH) by about 35 cm^{-1}, and the δ(CH) by about 25 cm^{-1}. It is probable that these changes are somehow related to the increased aromatic character of the molecule due to the deprotonation. Indeed, the π system is more delocalized on the imidazole ring in compound **II** than in compound **I**. The redistribution of the π system leads to slight changes of the bonds lengths. While the carbon−carbon bonds of the six-membered ring have a mean length of 1.406 Å in compound **I**, this value amounts to 1.413 Å in compound **II** which is consistent with a less pronounced double bond character.[37] Accordingly, a reinforcement of the double bond character is observed for the C_2-N_{13} and C_3-N_{11} bonds, whose lengths decrease from 1.400 Å to 1.394 and 1.386 Å, respectively. The weakened double bond character of the CC bonds explains the shift observed for the CH vibrations, as illustrated by the well-know sequence $\bar{\nu}$(≡C−H) > $\bar{\nu}$(═C−H) > $\bar{\nu}$(−C−H).

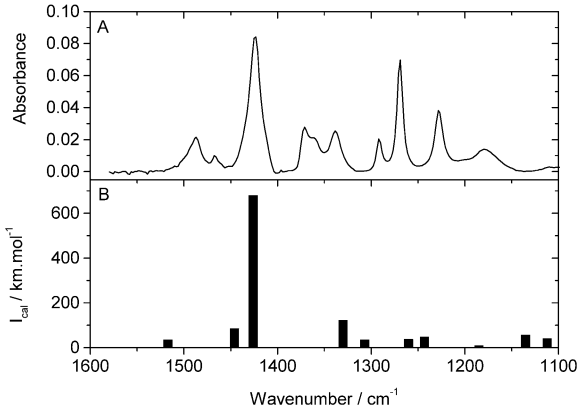

Figure 5. Comparison of the (A) experimental and (B) calculated spectra of anionic MBI, within the 1600−100 cm^{-1} range.

The change in the aromaticity of the molecule is further evidenced by the shift observed on the wavenumbers of the Q29, Q31, Q35, and Q39 modes. Those modes, which were assigned to out-of-plane skeletal deformations (torsion), undergo slight shifts (∼10 cm^{-1}) to higher wavenumbers upon deprotonation. It is then more difficult for the molecule to leave planarity in its anionic form than in its neutral one, as expected for an extended aromaticity.

Within the wavenumber range 1600−1100 cm^{-1}, which is experimentally accessible during the in situ measurements, the deprotonation of the MBI molecules results in considerable modifications of the spectrum. Since in this range the normal modes involve strong couplings, the spectral changes are attributed to a redistribution of the potential energy distributions of the normal modes. As can be shown in Figure 5, which presents the experimental and calculated spectra of anionic MBI, the DFT calculations fairly report these modifications, providing helpful information on the assignment of the experimental spectrum.

4.3. Gold−2-Mercaptobenzimidazole Compound. As was demonstrated in previous studies,[4,38] the reaction between MBI and gold implies the deprotonation of the molecule and the formation of a gold−sulfur bond. This reaction scheme, widely reported for thiols, is supported by different considerations, among them the report of Usón et al.[39] In their X-ray diffraction study of complexes of gold with different ligands including MBI, they demonstrated the coordination through the sulfur atom. According to Pearson's hard and soft acids and bases principle,[40−42] the higher softness of sulfur as compared to nitrogen[43] promotes the sulfur atom to a better interaction partner for the gold atom which in view of its size is a very soft metal atom. This is supported by the experimental hardness values of S, N, and Au, which amount to 4.14, 7.23, and 3.46 eV, respectively.[9] Similar observations were made by Tielens et al. in the study of the interaction between thiocyanate and silver surfaces.[16] They also pointed out that, in the thiocyanate anion SCN^-, the negative charge is preferentially located on the sulfur atom due to its greater softness. Finally, the very small difference in the electronegativity of Au and S is in favor of a covalent interaction between these atoms.

To examine how the coordination of MBI to gold affects its infrared spectrum, calculations were performed on a very simple model system involving only one gold atom interacting with MBI and corresponding to the structure **III** of Figure 2.

Depending on the initial atomic positions, two stable geometries were found, one with the gold atom in the plane of the molecule (*xy* plane on Figure 2) and the other one with the gold atom in the *xz* plane. The first structure was chosen, supported by the crystallographic data of Usón et al.[39] and by its lower energetic configuration.

The compound corresponding to the structure **III** belongs to the C_s point group so that 42 vibrations are expected and distributed as $\Gamma_{vib} = 29\ A' + 13\ A''$. Figure 6 compares the calculated spectra of the MBI and AuMBI compounds, split in different zones for clarity and presented in the stick form.

As expected, the coordination through the sulfur atom results in severe modifications of the modes involving the CS bond. The theoretical spectra predict a huge decrease of the intensities of the bands at 1180, 680, and 619 cm^{-1} and slight shifts for the bands at 473 and 419 cm^{-1}.

Due to the deprotonation of MBI upon reaction with gold, the modes involving the NH bonds are also strongly affected. Only one ν(NH) is observed at 3715 cm^{-1}, whose intensity is largely decreased. The Q16 mode of MBI at 1283 cm^{-1} has no equivalent in the AuMBI compound, which is consistent with its assignment to a δ(NH) vibration. The peaks at 645 and 621 cm^{-1} were assigned to the symmetric and antisymmetric τ(NH), respectively, this latter being infrared inactive due to its A_2 symmetry. The deprotonation causes the loss of one of these modes, explaining the absence of a band around 645 cm^{-1}. Simultaneously, the change in the symmetry of the molecule allows the observation of a band at 611 cm^{-1} assigned to the τ(NH) vibration. For the same reason of symmetry, the previously inactive A_2 mode at 590 cm^{-1} is predicted to become active.

Some modes are marginally affected by the coordination reaction. This is the case for the very intense peak at 782 cm^{-1}, characteristic of the τ(CH) vibrations of a 1,2-disubstituted benzene, for the ν(CH) vibrations around 3240 cm^{-1}, and for most of the bands located between 800 and 1150 cm^{-1}. Similarly, the bands at 1399, 1343, 1320, and 1250 cm^{-1} are preserved, although slight shifts are predicted.

Finally, the calculations predict a significant shift toward lower frequencies of the mode Q11 at 1515 cm^{-1}. The intensities of the mode Q9 and Q12 decreases, while the mode Q10 inactive for the pure MBI has a small intensity in the gold−MBI compound.

The DFT-calculated spectral modifications occurring upon coordination were compared to those observed in the experimental situation. The spectra A and B in Figure 7 are those of the MBI molecule and the AuMBI-1 compound, respectively. This AuMBI-1 compound is the reaction product of MBI with $AuCl_4^-$. The differences between the two spectra are in full agreement with those predicted by the calculations. Particularly noticeable are the complete extinction of the bands at 713 and 661 cm^{-1}, the presence of a new band at 621 cm^{-1}, and the huge decrease of the intensity of the band at 3154 cm^{-1}, which were associated with the deprotonation of molecule. The band at 1180 cm^{-1} is also strongly decreased, as was predicted.

One has to note that in the range 1700−1100 cm^{-1} the two spectra share a lot of common features. Devillanova and Verani made a similar observation concerning MBI and its reaction product with cadmium.[27] Interestingly, this wavenumber range corresponds to that which was experimentally accessible in our in situ-spectroelectrochemical (SNIFTIRS) measurements. The SNIFTIR spectrum of MBI adsorbed on a Au(111) surface obtained in our previous study[4] appeared to be very similar to that of AuMBI-1.

Since the theoretical spectrum of the compound **III**, calculated with a very simple model including only one gold atom, fairly agrees with the experimental spectra of both the AuMBI-1 compound and the self-assembled monolayer of MBI on a gold surface, it is strongly suggested that the vibrational properties

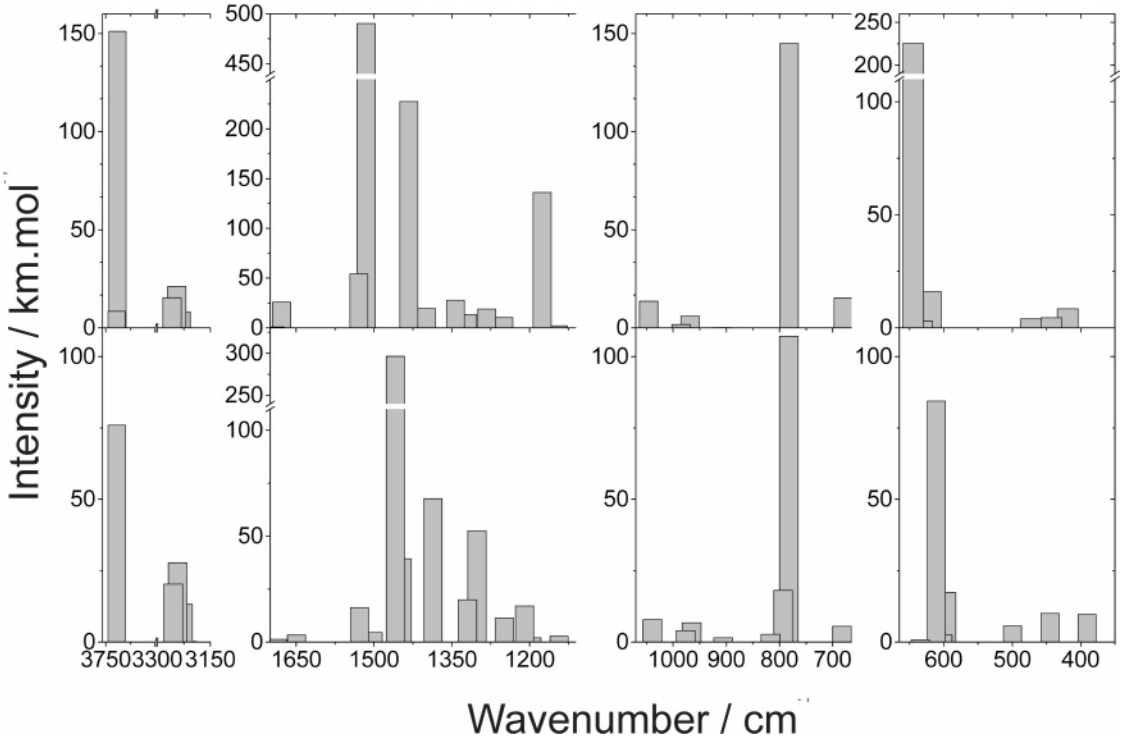

Figure 6. Comparison of the calculated spectra of (top) MBI and (bottom) AuMBI compound. The spectra were split in different wavenumber ranges for the sake of clarity.

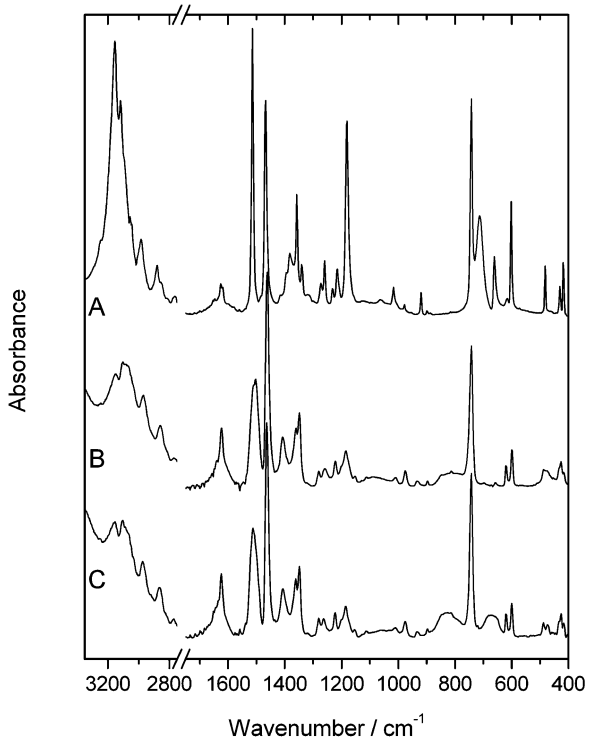

Figure 7. Experimental infrared absorption spectra of (A) solid MBI, (B) AuMBI-1 compound, and (C) AuMBI-2 compound.

of MBI in interaction with gold are essentially determined by the deprotonation and the coordination through the sulfur atom, regardless the size or geometry of the gold substrate and the extent of lateral interactions between MBI molecules.

This suggestion was further confirmed by the examination of the experimental spectrum, noted C in Figure 7, of the AuMBI-2 compound. This latter consists of small gold clusters covered by MBI and reflects then an intermediate situation between the AuMBI-1 compound (MBI in interaction with one gold atom) and the self-assembled monolayer of MBI on Au(111) (an organized monolayer of MBI molecules in interaction with an "infinite" gold surface with defined atomic structure). As can be seen on the figure, the experimental spectra of the AuMBI-1 and AuMBI-2 compounds are perfectly identical.

TABLE 2: Calculated Wavenumbers (in cm^{-1}) of Deuterated MBI (Structure I_b) and Deuterated Gold−MBI Compound (Structure III_b), in the Range 1250−1500 cm^{-1} [a]

	deuterated MBI (struct $\mathbf{I}_b$)		deuterated AuMBI (struct $\mathbf{III}_b$)
mode	$\bar{\nu}_{calc}/cm^{-1}$	$I_{calc}/km\cdot mol^{-1}$	$\bar{\nu}_{calc}/cm^{-1}$
Q10	1519	1	1519
Q9/Q11	1518	103	1493
Q9/Q11	1453	120	1448
Q12	1419	686	1418
Q13	1364	22	1364
Q14	1313	27	1313
Q15	1306	4	1294
Q17	1253	18	1243

[a] The calculated intensities (in $km\cdot mol^{-1}$) for deuterated MBI are also indicated.

4.4. Influence of Deuteration. As already mentioned in the Introduction, it is shown in Figure 1 that, within the range 1250−1500 cm^{-1}, the spectrum of deuterated MBI (compound $\mathbf{I}_b$) is very similar to that of the MBI adsorbed on Au(111) from deuterated water. Additionnaly, this experimental spectrum of deuterated MBI significantly differs from that of MBI.

The DFT calculations performed on compounds $\mathbf{I}_b$ and $\mathbf{III}_b$ fairly agree with these observations. The results are summarized in Table 2.

The band observed at 1415 cm^{-1} in the spectrum of deuterated MBI is undoubtfully assigned to the Q12 mode, regarding the excellent agreement between the experimental and calculated wavenumber and intensity. The absence in the experimental spectrum of bands corresponding to the modes Q10 and Q15 (and Q19) is supported by their corresponding calculated intensities which are very small. The bands located at 1223,

1346, and 1359 cm^{-1} are not affected by the deuteration. Calculations indicate that both Q9 and Q11 modes have a significant intensity, but only one band is experimentally observed, at 1472 cm^{-1}. Due to the strong couplings involved in these modes, it is not straightforward to definitely assign them.

In the entire spectral range, few other changes are however particularly noticeable. As expected, the NH vibrations are strongly shifted upon deuteration. The symmetric and antisymmetric NH strectchings are predicted to move from 3718 and 3715 cm^{-1} to 2734 and 2727 cm^{-1}, respectively, while the symmetric and antisymmetric out-of-plane bendings move from 645 to 468 cm^{-1} and from 621 to 475 cm^{-1}. As for the bands at 1180 and 1234 cm^{-1}, containing important contributions of in-plane NH bendings, they are shifted to 977 and 1036 cm^{-1}, respectively.

The fourth column of Table 2 presents the calculated wavenumbers of the deuterated gold−MBI compound $\mathbf{III}_b$. The very good correlation between these wavenumbers and those of compound $\mathbf{I}_b$ is highly consistent with the experimental similarities noted in Figure 1.

5. Conclusions

In situ infrared spectroscopy used in combination with electrochemical methods is a powerful technique for the examination of adsorbed organic layers. An accurate description of the interfacial structure requires precise information about the vibrational properties of the adsorbed molecules. Large molecules such as 2-mercaptobenzimidazole exhibit complex vibrational spectra. In addition to experimental data, DFT calculations allowed us obtaining a complete description of the 42 vibrational modes of MBI, as well as their symmetry. The structural modifications of the molecule led to spectral differences which were clearly assigned by comparing the MBI and MBI derivatives calculated spectra.

Additionally, DFT calculations provided new insights into the interaction of MBI with gold surfaces. For anionic MBI, the calculations demonstrate the localization of the negative charge on the sulfur atom, which strongly supports the previously proposed mechanism involving the deprotonation of the molecule and the coordination to gold through the sulfur. The formation of a gold−sulfur bond was further confirmed by the very good agreement between the calculated spectrum and the experimental spectra of different gold−MBI compounds. A very simple theoretical model with only one gold atom was used in this work. A more "realistic" model, including a gold cluster with a (111) surface termination and several MBI molecules would certainly provide a refinement to this work. However, such a system requires large computational capacity, and the gain of information for the interpretation of the experimental data will not be significant for this system. Our results have indeed shown that the vibrational properties of adsorbed MBI are essentially described by the coordination through the sulfur atom.

Acknowledgment. The ULB−VUB collaboration is performed under the auspices of the interuniversity Centre for Advanced Surfaces and Interfaces, Science and Engineering (CASIE). The authors are grateful to J. Liévin for helpful discussions. This work was supported by a grant from the "Fonds National de la Recherche Scientifique" (FRFC Project).

References and Notes

(1) Stole, S. M.; Popenoe, D. D.; Porter, M. D. Infrared Spectroelectrochemistry: a probe of the molecular architecture of the electrochemical interface. In *Electrochemical Interfaces: Modern techniques for in-situ interface characterization*; Abruna, H. D., Ed.; VCH: New York, 1992; p 339.

(2) Hoon-Khosla, M.; Fawcett, W. R.; Goddard, J. D.; Tian, W.-Q.; Lipkowski, J. *Langmuir* **2000**, *16*, 2356.

(3) Li, N.; Zamlynny, V.; Lipkowski, J.; Henglein, F.; Pettinger, B. *J. Electroanal. Chem.* **2002**, *524*−*525*, 43.

(4) Doneux, T.; Buess-Herman, C.; Lipkowski, J. *J. Electroanal. Chem.* **2004**, *564*, 65.

(5) Doneux, T.; Buess-Herman, C.; Hosseini, M. G.; Nichols, R. J.; Lipkowski, J. *Electrochim. Acta* **2005**, *50*, 4275.

(6) Alcolea Palafox, M.; Rastogi, V. K.; Tanwar, R. P.; Mittal, L. *Spectrochim. Acta, Part A* **2003**, *59*, 2473.

(7) Ramondo, F.; Pieretti, A.; Gontrani, L.; Bencivenni, L. *Chem. Phys.* **2001**, *271*, 293.

(8) Böhlig, H.; Ackermann, M.; Billes, F.; Kudra, M. *Spectrochim. Acta, Part A* **1999**, *55*, 2635.

(9) Parr, R. G.; Yang, W. *Density Functional Theory of Atoms and Molecules*; Oxford University Press: New York, 1989.

(10) Koch, W.; Holthausen, M. C. *A Chemist's Guide to Density Functional Theory*, 2nd ed.; Wiley-VCH: Weinheim, Germany, 2000.

(11) Perdew, J. P.; Wang, Y. *Phys. Rev. B* **1992**, *45*, 13244.

(12) Becke, A. D. *J. Chem. Phys.* **1993**, *98*, 5648.

(13) Hay, P. J.; Wadt, W. R. *J. Chem. Phys.* **1985**, *82*, 299.

(14) Wadt, W. R.; Hay, P. J. *J. Chem. Phys.* **1985**, *82*, 284.

(15) Hay, P. J.; Wadt, W. R. *J. Chem. Phys.* **1985**, *82*, 270.

(16) Tielens, F.; Saeys, M.; Tourwé, E.; Marin, G. B.; Hubin, A.; Geerlings, P. *J. Phys. Chem. A* **2002**, *106*, 1450.

(17) Blajiev, O.; Hubin, A.; Tielens, F.; Geerlings, P. *J. Raman Spectrosc.* **2003**, *34*, 295.

(18) Frisch, M. J.; Trucks, G. W.; Schlegel, H. B.; Scuseria, G. E.; Robb, M. A.; Cheeseman, J. R.; Zakrzewski, V. G.; Montgomery, J. A., Jr.; Stratmann, R. E.; Burant, J. C.; Dapprich, S.; Millam, J. M.; Daniels, A. D.; Kudin, K. N.; Strain, M. C.; Farkas, O.; Tomasi, J.; Barone, V.; Cossi, M.; Cammi, R.; Mennucci, B.; Pomelli, C.; Adamo, C.; Clifford, S.; Ochterski, J.; Petersson, G. A.; Ayala, P. Y.; Cui, Q.; Morokuma, K.; Malick, D. K.; Rabuck, A. D.; Raghavachari, K.; Foresman, J. B.; Cioslowski, J.; Ortiz, J. V.; Baboul, A. G.; Stefanov, B. B.; Liu, G.; Liashenko, A.; Piskorz, P.; Komaromi, I.; Gomperts, R.; Martin, R. L.; Fox, D. J.; Keith, T.; Al-Laham, M. A.; Peng, C. Y.; Nanayakkara, A.; Challacombe, M.; Gill, P. M. W.; Johnson, B.; Chen, W.; Wong, M. W.; Andres, J. L.; Gonzalez, C.; Head-Gordon, M.; Replogle, E. S.; Pople, J. A. *Gaussian98*; Gaussian, Inc.: Pittsburgh, PA, 1998.

(19) Martin, J. M. L.; El-Yazal, J.; Francois, J.-P. *Mol. Phys.* **1995**, *86*, 1437.

(20) De Proft, F.; Martin, J. M. L.; Geerlings, P. *Chem. Phys. Lett.* **1996**, *250*, 393.

(21) Form, G. R.; Raper, E. S.; Downie, T. C. *Acta Crystallogr., Sect. B* **1976**, *B32*, 345.

(22) Murty, V. V. S.; Murty, B. V. R. *Z. Kristallogr.* **1979**, *148*, 161.

(23) Ravikumar, K.; Mohan, K. C.; Bidyasagar, M.; Swamy, G. Y. S. K. *J. Chem. Crystallog.* **1995**, *25*, 325.

(24) Açikkalp, E.; Yildiz, K.; Yarligan, S.; Ogretir, C. *J. Mol. Struct. (THEOCHEM)* **2001**, *536*, 155.

(25) Szafran, M.; Koput, J.; Dega-Szafran, Z.; Pankowski, M. *J. Mol. Struct.* **2002**, *614*, 97.

(26) Cumper, C. W. N.; Pickering, G. D. *J. Chem. Soc., Perkin Trans. 2* **1972**, *14*, 2045.

(27) Devillanova, F. A.; Verani, G. *Aust. J. Chem.* **1980**, *33*, 279.

(28) Bigotto, A. *Spectrosc. Lett.* **1991**, *24*, 69.

(29) Periandy, B.; Mohan, S. *Asian J. Chem.* **1996**, *8*, 707.

(30) Harrison, D.; Ralph, J. T. *J. Chem. Soc. B* **1967**, 14.

(31) Rauhut, G.; Pulay, P. *J. Phys. Chem.* **1995**, *99*, 3093.

(32) Kalincsak, F.; Pongor, G. *Spectrochim. Acta A* **2002**, *58*, 999.

(33) Schrader, B. *Infrared and Raman Spectroscopy. Method and Applications*; VCH: Weinheim, Germany, 1995.

(34) Rao, C. N. R.; Venkataraghavan, R. *Spectrochim. Acta* **1962**, *18*, 541.

(35) Perrin, F. X.; Pagetti, J. *Corros. Sci.* **1998**, *40*, 1647.

(36) *Handbook of Chemistry and Physics*, 70th ed.; CRC Press: Boca Raton, FL, 1989.

(37) Pauling, L. *The Nature of the Chemical Bond*, 3rd ed.; Cornell University Press: Ithaca, NY, 1960.

(38) Whelan, C. M.; Smyth, M. R.; Barnes, C. J.; Brown, N. M. D.; Anderson, C. A. *Appl. Surf. Sci.* **1998**, *134*, 144.

(39) Uson, R.; Laguna, A.; Jimenez, J.; Gomez, M.; Sainz, A. *J. Chem. Soc., Dalton Trans.* **1990**, 3457.

(40) Pearson, R. G. *J. Am. Chem. Soc.* **1963**, *85*, 3533.

(41) Pearson, R. G. *Inorg. Chim. Acta* **1995**, *240*, 93.

(42) Geerlings, P.; De Proft, F.; Langenaeker, W. *Chem. Rev.* **2003**, *103*, 1793.

(43) De Proft, F.; Martin, J. M. L.; Geerlings, P. *Chem. Phys. Lett.* **1996**, *256*, 400.